Short Communication

Electrodeposition of Dendritic Silver Nanostructures and Their Application as Hydrogen Peroxide Sensor

Benzhi Liu[*]*, Min Wang*

School of Environmental Science and Engineering, Yancheng Institute of Technology, Yancheng, Jiangsu Province, China
[*]E-mail: benzhiliu@163.com

Well-defined dendritic silver nanostructures were successfully synthesized by electrodeposition method. The morphologies of the nanostructures and the crystal structure have been characterized by scanning electron microscopy and x-ray diffraction. The electrocatalytic activity of the dendritic silver nanostructures toward the electro-reduction of hydrogen peroxide has been examined by cyclic voltammetry and amperometric analysis. Based on this, electrochemical sensing of hydrogen peroxide was performed with a linear range of 4 µM to 36 µM and a detection limit of 0.9 µM.

1. INTRODUCTION

The determination of H_2O_2 is of great importance in environmental sciences and biochemistry as well as in food, pharmaceutical and clinical analysis [1–3]. Many analytical methods have been employed for the determination of H_2O_2, including titrimetry [4], spectrophotometry [5] and chemiluminescence [6]. In recent years, electrochemical detection of H_2O_2 attracted more attention because of its low detection limit, high sensitivity and simplicity [7, 8]. Compared to the extensive studies of enzyme-based H_2O_2 sensors, more and more attention has been focused on inorganic nanomaterials modified electrodes owing to their superior stability and convenience of electron transfer.

As a typical nanomaterial, silver has recently exhibited good catalytic activity for H_2O_2 and has attracted scientific interest [9, 10]. It is well-known that the morphologies of nanomaterials could affect their catalytic activity [11]. Dendritic structured materials have attracted much attention because of their fascinating hierarchical structures and potential applications in the catalysis and technological fields [12–14]. As electrode modification materials, dendritic structured materials have high specific

surface area along with numerous active sites and sharp edges which is critical for mass transfer and is in favor of heterogeneous catalysis [15]. Therefore, it is highly desirable to try dendritic silver nanostructures for H_2O_2 sensor fabrication.

Synthetic methods for dendritic silver nanostructures can be found mainly on electrochemical, chemical and physical means. Irradiations, chemical reagents and templates are usually used in their synthesis [16-18]. Electrodeposition is an efficient way to synthesize nanomaterials with high yields, and the nanomaterial shapes and sizes can be readily controlled by adjusting the preparation conditions [19]. Based on that, in our work, we synthesized a well-defined dendritic Ag nanostructures by electrodeposition. The dendritic structures were electrodeposited directly on the surface of the glassy carbon electrode. The electrocatalytic activity of the dendritic Ag structures towards H_2O_2 was evaluated with electrochemical techniques. The as-prepared silver nanostructures were used to construct a H_2O_2 sensor, which exhibited good electrocatalytic activity towards H_2O_2 reduction.

2. EXPERIMENTAL SECTION

2.1. Reagents and materials

Chemicals like $AgNO_3$, poly(vinylpyrrolidone) (PVP) and hydrogen peroxide (30%) were obtained from Sinopharm Chemical Reagent Co. Ltd. (China). All other reagents were of analytical grade and used without further purification. The electrodeposition solution containing 0.1 M KNO_3, 15 mM $AgNO_3$ and 20 mM PVP was prepared by dissolving 1.01g KNO_3, 0.255 g $AgNO_3$ and 0.222g PVP in 100 mL double distilled water. The 1 M H_2O_2 standard stock solution was prepared by diluting 10.2 mL H_2O_2 (30%) in 89.8 mL double distilled water. The 0.1M phosphate buffer solutions (PBS) at various pH values were prepared by mixing the stock solutions of NaH_2PO_4 and Na_2HPO_4, and then adjusting the pH with 0.1 M H_3PO_4 or NaOH. Doubly distilled water was used throughout the experiment.

2.2. Instrumentation

All electrochemical measurements were carried out on a CHI660 electrochemical workstation (ChenHua Instrument Company of Shanghai, China). A conventional three electrode system was used with a saturated calomel electrode (SCE, all potentials are given against this reference) as the reference electrode, a platinum wire as the counter electrode, and a modified glassy carbon electrode (GCE, 3mm in diameter) as the working electrode. Electrodeposition of dendritic silver nanostructures on glassy carbon electrode was accomplished by potentiostatic method at the potential of -0.4 V for 80s. The electrodeposition solution containing 0.1 M KNO_3 and 15 mM $AgNO_3$ in the presence of 20 mM PVP. The dendritic silver nanostructures were observed by S-3400N II scanning electron microscopy (SEM) (Hitachi, Japan). The phase structure of silver nanostructures was determined by X'TRA X-ray diffractometer (ARL, Switzerland).

3. RESULTS AND DISCUSSION

3.1. Characterization of the Ag nanostructures

Fig. 1 shows the low- and high-magnification SEM images of dendritic silver nanostructures. It can be observed that silver dendrites were obtained in a large quantity and good uniformity with open porous structure.
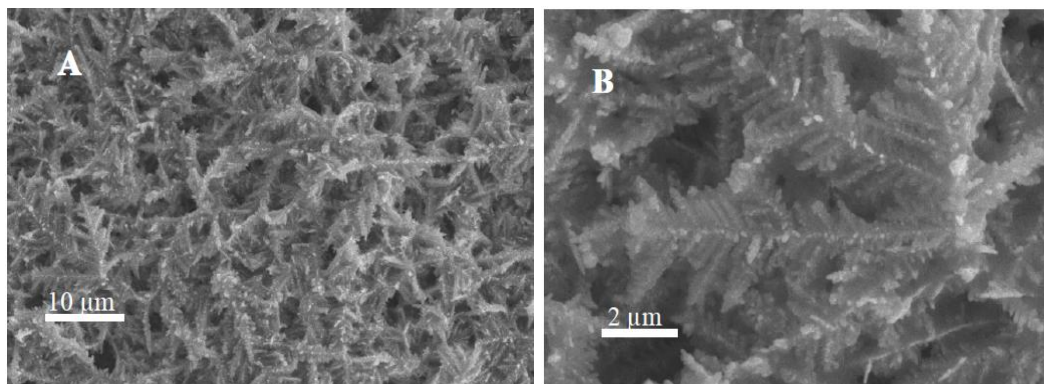

Figure 1. SEM images of dendritic silver nanostructures. Low- magnification (A) and high-magnification (B).
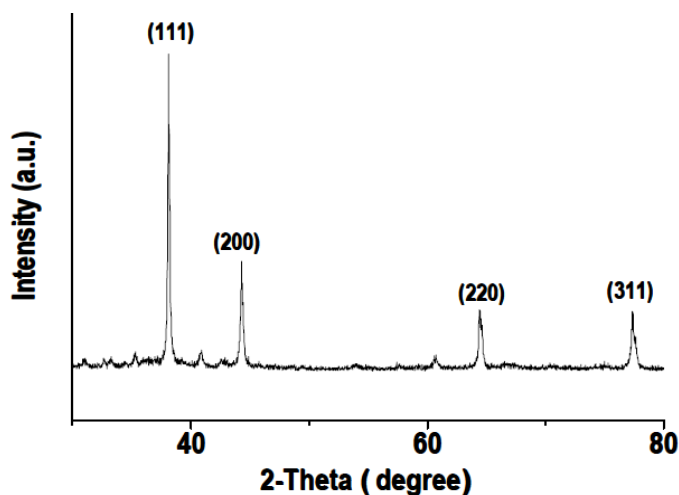

Figure 2. XRD patterns of dendritic silver nanostructures.

The individual Ag dendrites have two- and three- dimensional structures with one trunk and branches, which preferentially grow along two definite directions rather than randomly ramified growth. The branches are parallel to each other and in the same plane, and make an angle of about 60° with the trunk, forming symmetric structures. The diameter of the trunks is around 150- 250 nm and their length up to 5- 8 μm. The length of the branches can reach 1- 2μm. Interestingly, during the growth process of silver nanostructures, each branch can also be a trunk to support the growth of silver. Thus, the self-replication makes this kind of silver nanostructures have more advanced

structure. Fig. 2 shows the XRD patterns of the as-prepared silver nanostructures. In the XRD spectra, the four diffraction peaks at 2θ value of 38.1°, 44.2°, 64.4° and 77.4° could be indexed to the (1 1 1), (2 0 0), (2 2 0) and (3 1 1) diffraction peaks of the cubic structure of metallic Ag, indicating that the nanostructures is crystalline Ag [20].

3.2. Electrocatalytic properties towards H_2O_2.

The main electrocatalytic properties of the GCE modified with dendritic silver nanostructures(Ag/GCE) were demonstrated by cyclic voltammetry. A study to evaluate Ag/GCE response to H_2O_2 was carried out. Fig. 3A shows the cyclic voltammograms of GCE (a, c) and silver nanostructures modified GCE (b, d) in N_2-saturated 0.1 M PBS (pH 7.0) in the absence (a, b) and presence (c, d) of 10 mM H_2O_2. It can be seen that the reduction current on Ag/GCE is much larger than that of bare GCE and the peak potential appeared at around -0.55 V, indicating that dendritic silver nanostructures exhibit good electrocatalytic activity towards H_2O_2. The excellent catalytic activity of dendritic silver nanostructures could be attributed to the large surface area associated with the open porous structure, making them accessible to contact with the H_2O_2 substrate[10, 21].
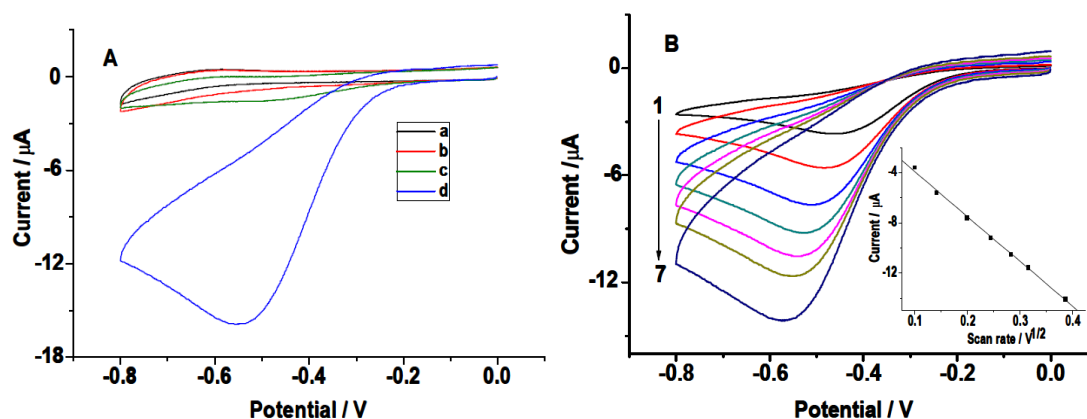

Figure 3. (A) Cyclic voltammograms of GCE (a, c) and silver nanostructures modified GCE (b, d) in N_2-saturated 0.1 M PBS (pH 7.0) in the absence (a, b) and presence (c, d) of 10 mM H_2O_2. Scan rate, 100 mV/s. (B) Cyclic voltammograms of silver nanostructures modified GCE in N_2-saturated 0.1 M PBS (pH 7.0) containing 5 mM H_2O_2 at different scan rates (1-7: 10, 20, 40, 60, 80, 100, and 150 mV/s). Inset: plot of peak current versus $v^{1/2}$.

The electrocatalytic behavior of the modified electrode at different scan rates were investigated. As shown in Fig. 3B, the reduction peak current increases with the increasing of scan rate. In the scan rate range of 10–150 mV/s, the peak current increases linearly with the square root of scan rate with a correlation coefficient of 0.9988 (inset in Fig. 3B), suggesting that the reaction is a diffusion-controlled process.

3.3. Amperometric sensor for H_2O_2 .

Fig. 4 shows a typical amperometric response of the Ag/GCE on successive addition of a certain amount of H_2O_2 into the stirring PBS (0.1 M, pH 7.0) at an applied potential of -0.55 V. Upon addition of H_2O_2, the current response reached 95% of the steady-state value within 5 s, indicating a fast amperometric response to H_2O_2 reduction. The amperometric response showed a linear relation with H_2O_2 concentration from 4 μM to 36 μM with a correlation coefficient of 0.9995 (inset in Fig. 4). The detection limit was 0.9 μM at a signal-to-noise ratio of 3, which was lower than that of some silver nanomaterials modified GC electrode [10, 21] and some HRP-based biosensors [22, 23].
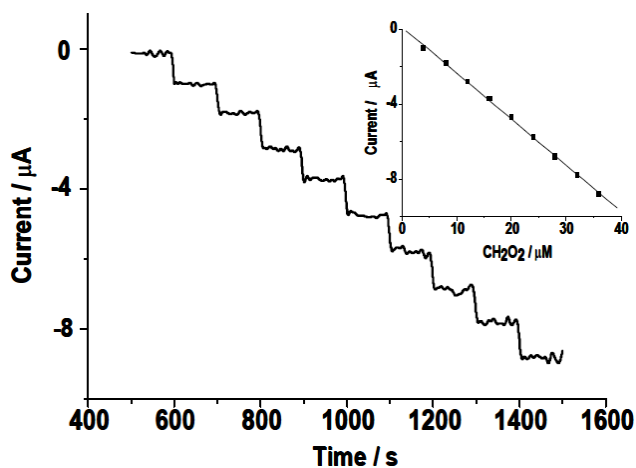

Figure 4. Amperometric response of the Ag/GC electrode towards successive addition of H_2O_2 in 0.1M PBS (pH=7.0) at − 0.55V vs. SCE. Inset: plot of current response vs. H_2O_2 concentrations.

The precision was evaluated by determinations of 20 μM H_2O_2 for five times using the same modified electrode. The fabrication reproducibility was estimated by detecting 20 μM H_2O_2 with five different modified electrodes made at the same procedure. The data were shown in table 1, which showing good precision and reproducibility. The long-term stability of the modified electrode was also investigated. The modified electrode was stored in PBS at 4 ∘C and measured intermittently, the current response to 20 μM H_2O_2 decreased less than 10% over one week.

Table 1. Evaluation of precision and reproducibility.

H_2O_2 concentration	H_2O_2 found	RSD (%) (n=5)
20 μM	19.8±0.2 μM	4.9
20 μM	20.1±0.4 μM	5.8

The selectivity of the sensor was evaluated. For the determination of 20 μM H_2O_2, no interference could be observed from glucose, uric acid, and ascorbic acid, which are at least 50 times more than H_2O_2. The result indicated that the sensor had an excellent selectivity for H_2O_2 detection.

As the proposed sensor has good selectivity, reproducibility and stability, the real sample of our laboratory waste water containing H_2O_2 was detected using the proposed sensor. The recovery experiment was carried out using the standard addition method. The analysis data for H_2O_2 were summarized in table 2. The results demonstrated potential application of this H_2O_2 sensor in real environmental samples.

Table 2. Analysis for H_2O_2 in waste water samples.

H_2O_2 in waste water	Added	H_2O_2 found	Recovery (%)	RSD (%) (n=5)
8.3 μM	5.0 μM	12.7±0.8 μM	95.5±6.0	5.9

4. CONCLUSION

In summary, dendritic Ag nanostructures were successfully obtained by electrodeposition and an electrochemical H_2O_2 sensor based on silver dendritic nanostructures was fabricated. The resulting sensor exhibits a fast amperometric response toward the H_2O_2 reduction together with a low detection limit. The current work provides a promising platform for fabricating nonenzymatic H_2O_2 sensors, and demonstrates that the electrodeposition is a simple method that may be extended to prepare various dendritic nanostructures from other noble metals.

References

1. P.N. Bartlett, P.R. Birkin, J.H. Wang, F. Palmisano and G.D. Benedetto, *Anal. Chem.* 70 (1998) 3685.
2. M.I. Prodromidis and M.I. Karayannis, *Electroanalysis*, 14 (2002) 241.
3. D.J. Barrington and A. Ghadouani, *Environ. Sci. Technol.*, 42 (2008) 8916.
4. D.R. Shankaran, K.I. Iimura and T. Kato, *Sens. Actuators B-Chem.*, 96(2003)523.
5. I.L.D. Mattos, L. Gorton and T. Ruzgas, *Biosens. Bioelectron.,* 18(2003)193.
6. C.G. Shi, Y. Shan, J.J. Xu and H.Y. Chen, *Electrochimica Acta,* 55(2010)8268.
7. J. Jia, B. Wang, A. Wu, G. Cheng, Z. Li and S. Dong, *Anal. Chem.,* 74(2002)2217.
8. X.L. Luo, J.J. Xu, Q. Zhang, G.J. Yang and H.Y. Chen, *Biosens. Bioelectron.,* 21(2005) 190.
9. C.M. Welch, C.E. Banks, A.O. Simm and R.G. Compton, *Anal. Bioanal. Chem.,* 382(2005) 12.
10. K. Cui, Y.H. Song, Y. Yao, Z.Z. Huang and L.Wang, *Electrochem. Commun.*, 10 (2008)663.
11. T.S. Ahmadi, Z.L. Wang, T.C. Green, A. Henglein and M.A. Elsayed, *Science,* 272 (1996) 1924.
12. Y. Zhou, S.H. Yu, C.Y. Wang, X.G. Li, Y.R. Zhu and Z.Y. Chen, *Adv. Mater.,* 11(1999)850.
13. R.Qiu, X.L. Zhang, R.Qiao, Y. Li, Y.I. Kim and Y.S. Kang, *Chem. Mater.,* 19 (2007) 4174.
14. X.P. Sun and M. Hagner, *Langmuir*, 23 (2007) 9147.

15. R. Qiu, H.G. Cha, H.B. Noh, Y.B. Shim, X.L. Zhang, R. Qiao, D. Zhang, Y.I. Kim, U.Pal and Y.S. Kang, *J. Phys. Chem. C,* 113 (2009) 15891.
16. Q. Yang, F. Wang, K. Tang, C. Wang, Z. Chen and Y. Qian, *Mater. Chem. Phys.,* 78 (2003) 495.
17. Y.C. Han, S.H. Liu, M. Han, J.C. Bao and Z.H. Dai, *Cryst. Growth Des.,* 9 (2009) 3941.
18. J.P. Xiao, Y. Xie, R. Tang, M. Chen and X.B. Tian, *Adv. Mater.*, 13 (2001) 1887.
19. G. Staikov, Wiley-VCH Verlag GmbH & Co. KGaA,Weinheim, 2007.
20. G.Wei, C. Nan, Y. Deng and Y. Lin, *Chem. Mater.,* 15 (2003) 4436.
21. Z.L. Liu, B. Zhao, Y. Shi, C.L. Guo, H.B. Yang and Z. Li, *Talanta,* 81 (2010) 1650.
22. H.S.Yin, S.Y. Ai, W.J. Shi and L.S. Zhu, *Sens. Actuators B-Chem.*, 137(2009)747.
23. C. Xiang, Y. Zou, L.X. Sun and F. Xu, *Sens. Actuators B-Chem.,* 136(2009)158.